

NOVEL METHOD FOR TRANSMISSION INFRARED ANALYSIS OF CLAY MINERALS USING SILICON WAFER SUBSTRATES

JEFFREY A. CAULFIELD, TODD A. WELLS AND KEITH E. MILLER*

Department of Chemistry and Biochemistry, University of Denver, 2190 East Iliff Ave., Denver, Colorado 80208, USA

Abstract—A novel method for the analysis of clay minerals using Fourier transform infrared spectroscopy is presented. Clay mineral suspensions are dried on a Si wafer substrate for transmission infrared (IR) analysis. Four natural Source Clays from the Source Clays Repository of The Clay Minerals Society, SWy-2, SAz-1, SHCa-1 and KGa-1b, as well as the synthetic hectorite, Laponite RD, were analyzed using the described method with signal to noise (s/n) ratios in excess of 100,000 for the strongly absorbing Si–O stretching frequency. Scanning electron microscopy (SEM) images show that the mineral films possess suitable uniformity and low surface roughness for transmission IR measurements that is confirmed by minimal deviations in the baseline of collected IR spectra. The IR spectra are generated and peak locations are compared to previously reported values, generated from KBr pellet and attenuated total reflectance methods.

Key Words—FTIR, Laponite, Silicon Wafer, Source Clays, Wafer Substrate.

INTRODUCTION

Infrared spectroscopy is a well established, useful and relatively economical tool for the characterization of clay minerals. The vibrational frequencies obtained from IR spectra can be used to deduce information about the mineral composition and structure (Farmer, 1974). Often, IR techniques are used in conjunction with other characterization techniques such as X-ray diffraction (XRD) for the determination of mineral group and type (Madejová and Komadel, 2001; Madejová, 2003). In addition to studying the mineral itself, IR methods are also employed to evaluate frequency shifts of sorbed analytes to help understand the adsorption mechanism of the compounds (de Oliveira, 2005; Kubicki *et al.*, 1997; Weissmahr *et al.*, 1997). It has also been shown that IR methods can be used quantitatively to show analyte adsorption on a clay mineral surface (Johnston *et al.*, 2002).

The IR spectra of clay minerals are typically obtained using various techniques such as attenuated total reflectance Fourier transform infrared (ATR-FTIR) spectroscopy, diffuse reflectance infrared Fourier transform spectroscopy (DRIFTS), and transmission IR through self-supporting clay films, mineral-containing KBr pellets, or glass slides (Madejová and Komadel, 2001; Farmer, 1974; Petit *et al.*, 2003). Each method possesses advantages and disadvantages depending on the specific needs of the study. The ATR-FTIR and DRIFTS capabilities are more expensive and less

commonly found compared to transmission FTIR instruments; however, they are capable of analyzing a wide range of mineral samples with little sample preparation. Self supporting clay films and KBr pellets can be time consuming to produce and tend to require more skill in order to produce useful spectra, but can be analyzed using more economical instrumentation.

The method presented here describes a technique for generating a thin mineral film that is well suited for absorbance measurements in transmission mode for the mid-IR region. The mineral film is generated on an optical-grade Si wafer where film thickness can be easily adjusted. Transmission IR through Si wafers is an established technique in materials-development research intended for the semiconductor industry (Lau *et al.*, 2000a, 2000b), but has not appeared to date in the clay-mineral literature. Silicon wafers are economical substrate choices that are reusable and sufficiently transparent in the mid-IR region to determine the absorption behavior of a mineral. Conceptually, a similar method was reported by Hunt *et al.* (1950) where mineral films were applied to salt windows for transmission IR analysis. The films were generated by smearing mineral pastes containing non-aqueous solvents on the salt window; however, the dried films possessed surface roughness sufficient to scatter the IR source light, thus causing significant baseline shifts.

The method reported here offers an analytical alternative to the previously mentioned methods with several benefits. First, IR absorption instrumentation in transmission mode is more commonly found in research laboratories compared to ATR and DRIFTS capabilities, increasing its widespread appeal. Second, our experience shows that sample preparation is less time-intensive and requires less skill than self-supporting film methods.

* E-mail address of corresponding author:

kmiller3@du.edu

DOI: 10.1346/CCMN.2007.0550210

Third, this method allows for the characterization of nano-sized clay minerals such as the synthetic clay, Laponite RD, with a non-polarized source light. Fourth, in some applications it may be useful to perform both transmission IR and XRD analysis on the same sample. It has been shown previously that XRD analysis can be performed on Si wafers, a single crystal mount where the Si peak provides a useful internal standard (Eberl *et al.*, 1998; Queralt *et al.*, 2001; Dudek *et al.*, 2002). Finally, this method provides for a simple, but effective alternative to probe the Si–O vibrations on thin clay films that have been saturated with alkali metals. (Karakassides *et al.*, 1999a, 1999b)

This study describes the method for IR absorption analysis in detail and demonstrates its usefulness using several source clays from the Source Clays Repository. The instrumental noise, n , for various wavelength regions that are of interest to the clay mineralogical community are calculated for two types of doped silicon wafers to aid interested readers in substrate selection.

MATERIALS AND METHODS

Materials

Wyoming montmorillonite (SWy-2), Arizona montmorillonite (SAz-1), California hectorite (SHCa-1) and Georgia kaolinite (KGa-1b) were purchased from the Source Clays Repository of The Clay Minerals Society at Purdue University (West Lafayette, Indiana). Laponite RD was obtained from Southern Clay Products, Inc. (Gonzales, Texas). Potassium hydroxide (KOH) solution, 50% (w/v), was purchased from Fisher Scientific Corporation (Fairlawn, New Jersey). Ultrapure deionized (DI) water with $>18 \text{ M}\Omega \text{ cm}$ (25°C) resistivity was produced by filtering house DI water with a Milli-Q Water System from Millipore (Billerica, Massachusetts). Mineral substrates were generated from two types of Si wafers referred to herein as n-type or p-type. The n-type wafers were obtained through Wafer Net, Inc. (San Jose, California), whereas the p-type wafers were purchased from Montco Silicon Technologies, Inc. (Spring City, Pennsylvania). Wafer specifications are listed in Table 1.

Table 1. Specifications for the wafers used in this study.

	Wafer specifications	
	n-type	p-type
Crystal growth method	CZ ¹	CZ ¹
Diameter	100 mm	3 inch
Crystal orientation	<100>	<100>
Thickness	356–406 μm	350–550 μm
Dopant	Sb	P
Resistivity	10–20 $\Omega \text{ cm}$	0.001–0.09 $\Omega \text{ cm}$

¹CZ = Czochralski crystal growth

Sample preparation

The naturally occurring Source Clays were prepared for analysis by suspending 10 g of as received material in 1 L of ultrapure DI water. Prior to fractionation, five drops of 50% (w/v) KOH were added to the KGa-1b suspension in order to disrupt clay conglomerates (Burgos *et al.*, 2002). The $<2 \mu\text{m}$ Stokes diameter fraction was then separated using a Sorvall RC5CPlus centrifuge (Thermo Electron Corporation, Asheville, North Carolina) and collected. All fractionations were performed using a Sorvall GSA rotor with 250 mL polycarbonate centrifuge bottles (manufactured by Nalgene and purchased from VWR International, West Chester, Pennsylvania). The fractionated minerals were subsequently freeze dried using a Benchtop 3.3/Vacu-Freeze system (Virtis Company, Gardiner, New York) and stored until needed for experiments. Laponite RD was used as received.

Seven n-type Si wafer substrates of near square geometry were generated by cleaving one 100 mm diameter wafer using a diamond-tipped scribe. The square substrates were typically between 2.5 and 3.5 cm in dimension. One of the seven squares was set aside as a dedicated background for IR studies whereas the remaining six squares were used as substrates for the mineral samples. Typically, five sections were obtained from the 3 inch p-type wafers that were used for analysis of wafer transparency and noise calculations.

The dried mineral was added to DI water to generate suspensions typically between 0.1 and 0.2% (w/w). 1.5 mL aliquots of the suspensions were placed on the wafer substrates and allowed to air dry in a temperature controlled, environmental chamber. Once dry, the wafers were mounted on sample cards (International Crystal

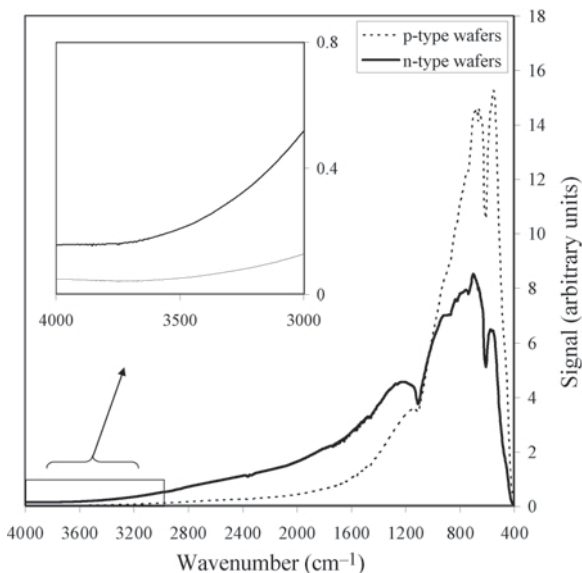


Figure 1. Single beam spectrum for n-type and p-type wafers.

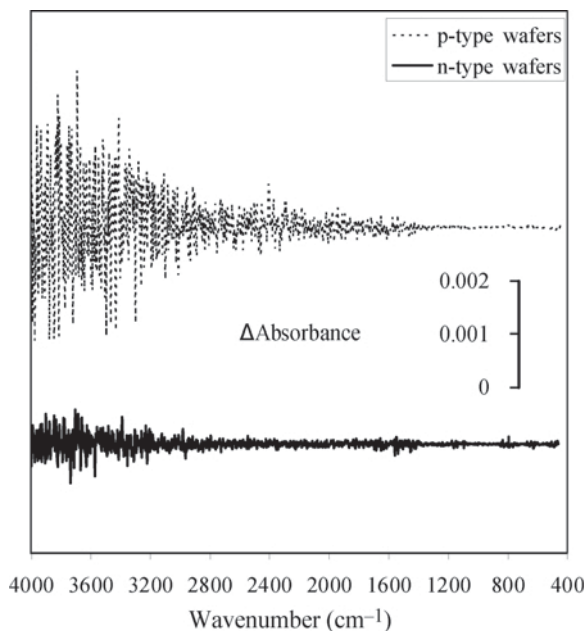


Figure 2. Instrument absorbance noise from blank n-type and p-type wafers.

Laboratories, Garfield, New Jersey) and inserted into the sample holder for transmission IR studies.

Sample characterization

Transmission FTIR was performed using a Digilab FTS 7000 FTIR spectrometer (Digilab, Massachusetts) equipped with a liquid nitrogen-cooled, broadband mercury cadmium telluride (MCT) detector. A blank wafer was used as the background and spectra were collected for 512 scans at a resolution of 4 cm^{-1} between 400 and 4000 cm^{-1} . Signal noise, as a function of wavenumber, was determined by taking background and absorption spectra of the same blank wafer, then performing a baseline correction to account for any minor deviations from zero absorbance. The absorbance noise value, reported at a particular wavenumber, was

Table 2. Calculated instrument noise at selected wavenumbers for both n-type and p-type wafers.

Wavenumber (cm^{-1})	Instrumental noise, n (Abs)	
	n-type	p-type
3500	8.96E-04	1.75E-04
3000	3.60E-04	1.09E-04
2500	2.23E-04	4.05E-05
2000	1.43E-04	3.47E-05
1500	4.67E-05	4.32E-05
1000	6.34E-06	1.03E-05
500	9.79E-06	2.83E-05

determined by calculating the standard deviation of 21 points centered at the particular wavenumber. For clay mineral analysis, sample mounts were prepared such that the maximum absorbance, a result of the Si–O stretching frequency between 1000 and 1050 cm^{-1} , ranged from 0.77 to 1.32 absorbance units. The IR absorption spectra are presented with the maximum absorption normalized to 1. Mineral IR spectra were not baseline corrected. Scanning electron microscopy was performed using a JEOL 5800LV system (JEOL Ltd., Tokyo, Japan) using the secondary electron detector. Samples were coated with a thin layer of gold prior to imaging.

RESULTS AND DISCUSSION

Signal and instrumental noise analysis

The single-beam spectra for the p-type and n-type wafers are shown in Figure 1. The n-type wafers used in this study allow more source light through the sample at wavenumbers $>1100\text{ cm}^{-1}$ when compared to the p-type wafers. Thus, the n-type wafers were selected for the analysis of clay minerals (discussed later in this paper) due to the increased light intensity in the 1100 – 4000 cm^{-1} region, where several absorption bands of the minerals occur. Figure 2 graphically demonstrates the instrumental

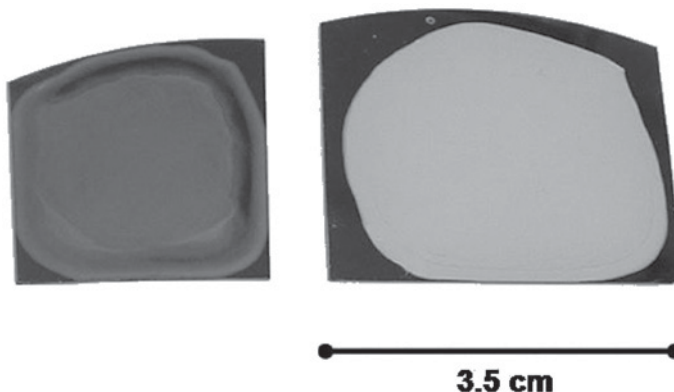


Figure 3. Thin SWy-2 films after the air-drying process from 0.1% (w/w) (left) and 0.5% (w/w) (right) solutions. The dried films are on the cleaved Si wafer substrates.

Table 3. Signal to noise (s/n) ratio of a SWy-2 sample for selected IR absorption bands.

Wavenumber (cm^{-1})	Raw signal (abs)	n (abs)	s/n
3630	0.138	2.20E-04	6.27E+02
1626	0.020	4.30E-05	4.60E+02
1046	0.765	6.00E-06	1.28E+05

Sample was generated from a 0.1% (w/w) solution dried on an n-type wafer.

noise for the two wafer backgrounds, whereas Table 2 provides the calculated noise at selected wavenumbers. As expected, the noise levels decrease with decreasing wavenumber resulting from the increase in source light intensity. From Table 2 it can be seen that an absorbance of 1 would correspond to a signal to noise (s/n) ratio ranging between 1000 and 100,000 depending on peak location for the n-type wafers.

Characterization of clay films

Figure 3 shows a photograph of two SWy-2 samples prepared from 0.1% and 0.5% (w/w) solutions. A visual inspection shows uniform mineral coverage with sufficient area to correspond to the 1.2 cm spot size from the light source of the instrument used. For this study, films generated using 0.1% to 0.2% (w/w) clay solutions

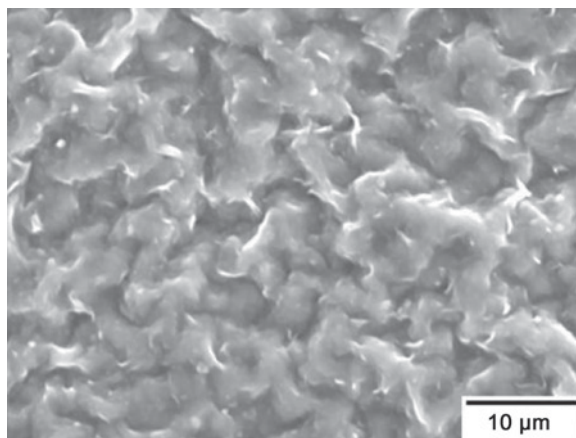


Figure 4. Representative SEM image from a 0.5% (w/w) SWy-2 solution air dried on a Si wafer substrate.

generated a maximum absorbance between 0.77 and 1.32 arising from the stretching frequency of Si–O. Thicker films can easily be produced by increasing the solution weight percent for analysis of weaker absorption features.

Figure 4 shows a representative SEM image for the surface of a SWy-2 sample prepared on a Si wafer. The SEM shows uniformity and surface roughness on the scale of microns. Laponite RD films generated on Si wafers are visually transparent suggesting no surface

Table 4. Peak assignments and positions from SWy-2 and SAz-1 montmorillonites.

Peak assignment ²	SWy-2			SAz-1		
	Si wafer ¹	Wavenumber (cm^{-1}) KBr ²	ATR ²	Si wafer ¹	Wavenumber (cm^{-1}) KBr ²	ATR ²
OH stretching of structural hydroxyl groups	3630	3632	–	3621	3622	–
OH stretching of structural hydroxyl groups	–	3627	3626	–	3620	3610
OH stretching of water	–	3422	3393	–	3426	3373
OH deformation of water	1626	1634	1632	1627	1634	1629
Si–O stretching (longitudinal mode)	1114	–	1116	–	–	1102
Si–O stretching	1046	1041	1003	1033	1030	992
AlAlOH deformation	920	917	916	920	915	913
AlFeOH deformation	886	885	885	–	–	–
AlMgOH deformation	852	842	846	842	842	837
Si–O stretching of quartz and silica	799	798	797	–	–	–
Si–O stretching of silica	–	–	–	–	792	798
Si–O stretching of quartz	779	778	779	–	–	–
Si–O	–	–	687	–	–	684
Coupled Al–O and Si–O, out-of plane	–	620	623	627	620	617
Al–O–Si deformation	523	524	–	519	520	–
Si–O–Si deformation	465	466	–	464	465	–

¹ This study

² Madejová and Komadel (2001)

Data collected using FTIR in transmission mode through Si wafers and compared to previously reported ATR and KBr pellet values.

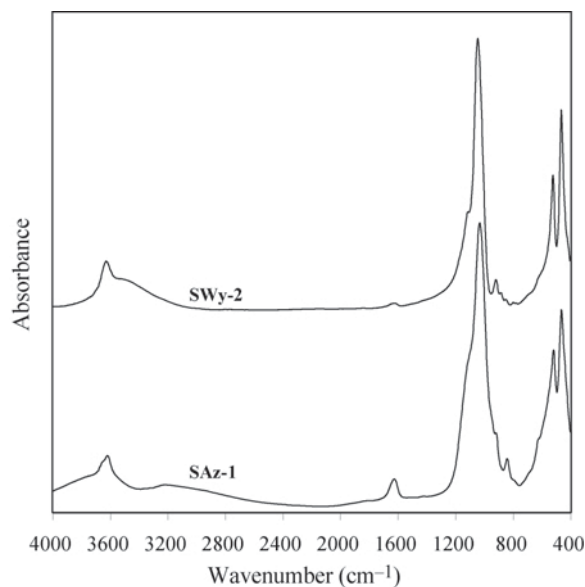


Figure 5. Absorbance-normalized FTIR spectra from a 0.1% (w/w) SWy-2 and 0.2% (w/w) SAz-1 suspension, air dried on a Si wafer substrate.

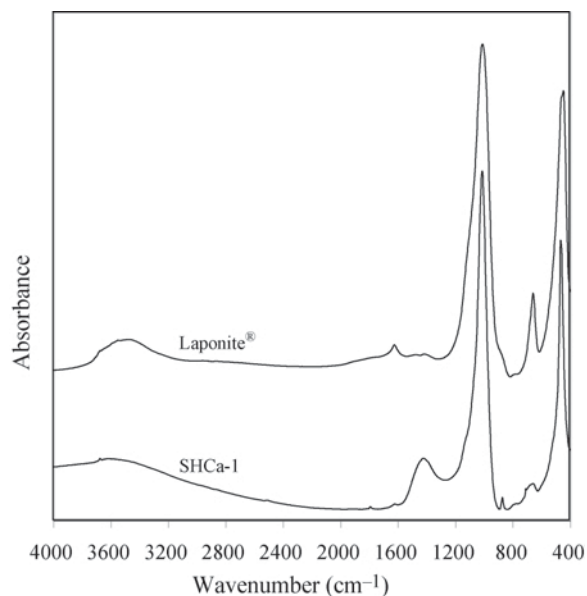


Figure 6. Absorbance-normalized FTIR spectra from a 0.1% (w/w) Laponite RD and 0.1% (w/w) SHCa-1 suspension, air dried on a Si wafer substrate.

features large enough to scatter visible light. Further characterization of a Laponite RD film using SEM analysis was unable to determine any surface features, suggesting a particularly smooth surface.

Infrared analysis

Data generated in this study are compared to those previously published by Madejová and Komadel (2001) where KBr pellet and ATR methods were primarily

employed. Their work showed peak locations and assignments for several Source Clays, including the four naturally occurring minerals used in this study. Tabular comparisons are made between the spectra generated by the method described here and the spectra presented and peak assignments determined by Madejová and Komadel. Transmission IR analysis of two Source Clay montmorillonites (SWy-2 and SAz-1) are presented in Figure 5. General peak locations are in

Table 5. Peak assignments and positions for Laponite RD and California hectorite (SHCa-1).

Peak assignment ²	SHCa-1			Laponite RD Wavenumber (cm ⁻¹) Si wafer ¹
	Si wafer ¹	Wavenumber (cm ⁻¹) KBr ²	ATR ²	
OH stretching of structural hydroxyl groups	3677	3678	3675	3679
OH stretching of bonded water	—	—	3629	—
OH stretching of water	3479	3438	3402	3475
Combination band of calcite	1793	1798	—	—
OH deformation of water	1623	1630	1633	1627
CO ₃ stretching of calcite	1423	1430	1421	—
Si—O stretching	1015	1013	989	1013
Out-of-plane bending of calcite	874	875	874	—
Si—O of silica	777	800	795	—
Si—O stretching and in-plane bending of calcite	711	710	701	—
Mg ₃ OH deformation	662	656	651	660
Mg—O stretching out of plane	—	524	—	—
Si—O—Si deformation	468	468	—	449

¹ This study

² Madejová and Komadel (2001)

Data collected using FTIR in transmission mode through Si wafers. Comparison values for SHCa-1 reported previously using ATR and KBr pellet methods.

agreement with those determined by the ATR and KBr methods. Table 3 shows the s/n ratio for three distinct peaks at different locations from the SWy-2 spectra. The s/n ratio is clearly much larger for the OH-stretching peak at 3630 cm^{-1} due to the large signal and minimal noise; however, the small peak at 1626 cm^{-1} with a s/n ratio of 460 is still easily identified.

Table 4 shows peak assignments for the montmorillonite Source Clays with the corresponding peak locations. Peak locations are expected to align better with the KBr data than with the ATR data due to frequency shifts arising from the optical physics of an ATR system (Urban, 1996; Graf *et al.*, 1987; Rintoul *et al.*, 1998). The OH deformation of water on SWy-2 at 1626 cm^{-1} determined by this study is shifted to a lower energy compared to the results of KBr and ATR analysis (1634 and 1632 cm^{-1} , respectively). This would suggest that the adsorbed water on the mineral surface is less hindered when dried on the wafer than in the KBr and ATR systems (Farmer, 1974).

Figure 6 and Table 5 correspond to the natural and synthetic hectorites, SHCa-1 and Laponite RD, respectively. Similar to the montmorillonite samples discussed above, peak locations are in general agreement with previously published literature (Madejová and Komadel, 2001). The SHCa-1 sample also shows lower absorption energy for deformation of adsorbed water (1623 cm^{-1}) compared to KBr and ATR methods. This method is particularly useful for generating IR spectra of clay

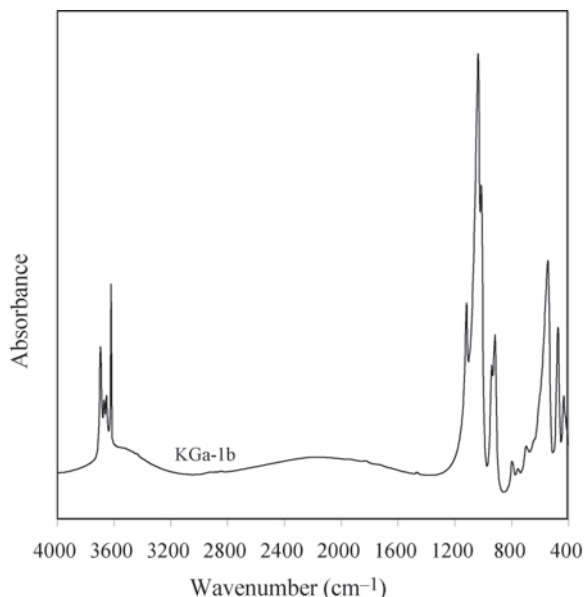


Figure 7. Absorbance-normalized FTIR spectrum from a 0.1% (w/w) KGa-1b suspension, air dried on a Si wafer substrate.

minerals such as Laponite that have individual platelet dimensions on the order of 20–30 nm (Neumann and Sansom, 1970). The platelet size is too small to generate self-supporting films successfully from such minerals. The ATR can be used to generate such data; however, our experience shows that generating sufficient signal

Table 6. Peak assignments and positions for Georgia kaolinite (KGa-1b).

Peak assignment ²	KGa-1b		
	Si wafer ¹	Wavenumber (cm ⁻¹) KBr ²	ATR ²
OH stretching of inner-surface hydroxyl groups	3695	3694	3689
OH stretching of inner-surface hydroxyl groups	3669	3669	3669
OH stretching of inner-surface hydroxyl groups	3653	3653	3651
OH stretching of inner hydroxyl groups	3620	3620	3619
OH stretching of water	3437	3457	–
OH deformation of water	–	1635	–
Si–O stretching (longitudinal mode)	1117	–	1115
Perpendicular Si–O stretching	–	1102	–
In-plane Si–O stretching	1035	1033	1027
In-plane Si–O stretching	1012	1011	1005
OH deformation of inner-surface hydroxyl groups	940	938	937
OH deformation of inner hydroxyl groups	916	915	912
Si–O	797	791	788
Si–O, perpendicular	754	755	751
Si–O, perpendicular	696	697	681
Si–O	–	–	645
Al–O–Si deformation	544	541	–
Si–O–Si deformation	472	472	–
Si–O deformation	433	432	–

¹ This study

² Madejová and Komadel (2001)

Data collected using FTIR in transmission mode through Si wafers and compared to previously reported ATR and KBr pellet values).

can be difficult due to the limited penetration of the evanescent wave in the ATR system.

Figure 7 and the corresponding Table 6 show the IR spectrum and data for KGa-1b. The multiple peaks, characteristic of kaolinite-type clay, seen in the regions of 3600–3700 cm^{-1} and 900–1200 cm^{-1} can easily be distinguished.

The authors recognize that much of the s/n discussion in this paper is dependent on the particular instrument in use. These spectra have been reproduced on more economical IR instrumentation used in undergraduate teaching laboratories with success (data not shown for brevity). Thus, in addition to research applications, the method reported here can also find application in undergraduate and graduate teaching environments. In addition, due to the non-destructive nature of IR, this method benefits from the possibility of performing other types of analysis, such as XRD, on the same sample.

CONCLUSIONS

A novel method for creating thin clay films for analyzing clay minerals by transmission IR techniques is presented. Clay suspensions dried on a Si wafer were reproducible, provide good s/n ratios and generate minimal deviation of the IR baseline. The IR spectra are in excellent agreement with other analytical techniques used to evaluate clay minerals and absorbance values can easily be adjusted by increasing the clay concentration in the suspension before drying.

ACKNOWLEDGMENTS

Funding for this project was provided by various University of Denver sources including the Department of Chemistry and Biochemistry, the Faculty Research Fund and the Professional Research Opportunity Fund. The authors gratefully acknowledge Southern Clay Products, Inc. for their donation of the Laponite RD material and the discussions with Dr Donald Stedman.

REFERENCES

Burgos, W.D., Pisutpaisal, N., Mazzarese, M.C. and Chorover, J. (2002) Adsorption of quinoline to kaolinite and montmorillonite. *Environmental Engineering Science*, **19**, 59–68.

de Oliveira, M., Johnston, C.T., Premachandra, G.S., Teppen, B.J., Li, H., Laird, D.A., Zhu, D. and Boyd, S.A. (2005) Spectroscopic study of carbaryl sorption on smectite from aqueous suspension. *Environmental Science & Technology*, **39**, 9123–9129.

Dudek, T., Śródoń, J., Eberl, D.D., Elsass, F. and Uhlik, P. (2002) Thickness distribution of illite crystals in shales. I: X-ray diffraction vs. high-resolution transmission electron microscopy measurements. *Clays and Clay Minerals*, **50**, 562–577.

Eberl, D.D., Nuesch, R., Šucha, V. and Tshipursky, S. (1998) Measurement of fundamental illite particles thickness by X-ray diffraction using PVP-10 intercalation. *Clays and Clay Minerals*, **46**, 89–97.

Farmer, V.C. (1974) *The Infrared Spectra of Minerals*. Monograph 4, Mineralogical Society, London, pp. 1, 11–25, 306–309, 352–353.

Graf, R.T., Koenig, J.L. and Ishida, H. (1987) Comparison of FT-IR transmission, specular reflectance, and attenuated total reflectance spectra of polymers. Pp. 385–395 in: *Fourier Transform Infrared Characterization of Polymers* (H. Ishida, editor). Plenum Press, New York.

Hunt, J.M., Wifherd, M.P. and Bonham, L.C. (1950) Infrared absorption spectra of mineral and other inorganic compounds. *Analytical Chemistry*, **22**, 1478–1497.

Johnston, C.T., Sheng, G., Teppen, B.J., Boyd, S.A. and de Oliveira, M.F. (2002) Spectroscopic study of dinitrophenol herbicide sorption on smectite. *Environmental Science & Technology*, **36**, 5067–5074.

Karakassides, M.A., Gournis, D. and Petridis, D. (1999a) An infrared reflectance study of Si-O vibrations in thermally treated alkali-saturated montmorillonites. *Clay Minerals*, **34**, 429–438.

Karakassides, M.A., Madejová, J., Arvaiová, B., Bourlinos, A., Petridis, D. and Komadel, P. (1999b) Location of Li(I), Cu(II), and Cd (II) in heated montmorillonite: evidence from specular reflectance infrared and electron spin resonance spectroscopies. *Journal of Materials Chemistry*, **9**, 1553–1558.

Kubicki, J.D., Itoh, M.J., Schroeter, L.M. and Apitz, S.E. (1997) Bonding mechanism of salicylic acid adsorbed onto illite clay: An ATR-FTIR and molecular orbital study. *Environmental Science & Technology*, **31**, 1151–1156.

Lau, K.K.S., Caulfield, J.A. and Gleason, K.K. (2000a) Structure and morphology of fluorocarbon films grown by hot filament chemical vapor deposition. *Chemistry of Materials*, **12**, 3032–3037.

Lau, K.K.S., Caulfield, J.A. and Gleason, K.K. (2000b) Variable angle spectroscopic ellipsometry of fluorocarbon films from hot filament chemical vapor deposition. *Journal of Vacuum Science & Technology A*, **18**, 2404–2411.

Madejová, J. (2003) FTIR techniques in clay mineral studies. *Vibrational Spectroscopy*, **31**, 1–10.

Madejová, J. and Komadel, P. (2001) Baseline studies of The Clay Minerals Society Source Clays: Infrared methods. *Clays and Clay Minerals*, **49**, 410–432.

Neumann, B.S. and Sansom, K.G. (1970) The study of gel formation and flocculation in aqueous clay dispersions by optical and rheological methods. *Israel Journal of Chemistry*, **8**, 315–322.

Petit, S., Decarreau, A. and Righi, D. (2003) The use of glass slide clay-deposit for IR spectroscopy. *Comptes Rendu Geoscience*, **335**, 737–741.

Queralt, I., Sanfeliu, T., Gomez, E. and Alvarez, C. (2001) X-ray diffraction analysis of atmospheric dust using low-background supports. *Aerosol Science*, **32**, 453–459.

Rintoul, L., Panayiotou, S.K., George, G., Cash, G., Frost, R., Bui, T. and Fredricks, P. (1998) Fourier transform infrared spectrometry: a versatile technique for real world samples. *Analyst*, **123**, 571–577.

Urban, M.W. (1996) *Attenuated Total Reflectance Spectrometry of Polymers: Theory and Practice*. American Chemical Society, Washington, D.C. pp. 49–70.

Weissmahr, K.W., Haderlein, S.B. and Schwarzenback, R.P. (1997) In situ spectroscopic investigations of adsorption mechanism of nitroaromatic compounds at clay minerals. *Environmental Science & Technology*, **31**, 240–247.

(Received 8 May 2006; revised 14 December 2006; Ms. 1171; A.E. Peter Komadel)